

Statistical analysis for discrimination of prompt gamma ray peak induced by high energy neutron: Monte Carlo simulation study

Moo-Sub Kim, Joo-Young Jung, and Tae Suk Suh

Department of Biomedical Engineering and Research Institute of Biomedical Engineering, College of Medicine, Catholic University of Korea, Seoul 505, Korea

*Corresponding author: suhsanta@catholic.ac.kr

1. Introduction

The purpose of this research was the statistical analysis for discrimination of the prompt gamma ray peak induced by the 14.1 MeV neutron particles from spectra using Monte Carlo simulation [1]. For the simulation, the information of the eighteen detector materials was used to simulate spectra by the neutron capture reaction.

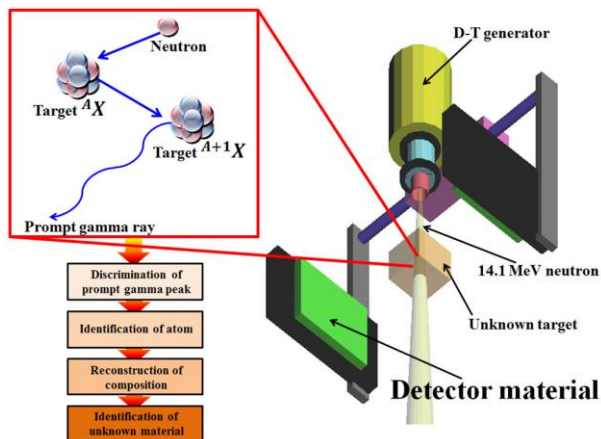


Fig. 1. Diagram of simulation of prompt gamma ray activation analysis (PGAA). The information of several detector materials was used to simulate the prompt gamma ray spectra.

2. Methods and Results

The geometry of the D-T generator and the detector were referred from other research. The detector size (50 cm × 50 cm × 8 cm) was fixed to maintain the identical physical factors excluding the materials. The area size of the detector was referred from the specification of actual instruments which is used to the PGAA at the harbor or the airport. However, in order to increase the counts number of the gamma ray, the thickness of the detector was set thicker than conventional instruments [2]. The distance between neutron source and the center of target was set at the 100 cm, and the distance between detector and target was defined as the 50 cm. The neutron particle can induce the prompt gamma ray

by the nuclear reaction with atoms. As the Fig. 1, because this prompt gamma ray has distinct characteristic atom by nuclide, the component of target material can be identified using the prompt gamma ray peak analysis. Basically, in order to simulate interaction between the material for the gamma ray detection and the photon, the physical and chemical characteristic information of the material for gamma ray detection, such as the density, ratio of the composition atom, and interaction characteristic with the photon, etc., are required. There are two major detector materials (a scintillator and a semiconductor) for the simulation in this study, and the physical and chemical characteristic information of the detector material was inserted to the each simulation. To use Gaussian energy broadening (GEB) function in the MCNPX code, the solutions of the dual equations of full width at half maximum (FWHM) (Eq. (1)) were obtained using the average energy resolution value at the 511 keV and 662 keV, respectively [3].

$$FWHM = a + b\sqrt{E} \quad (1)$$

a= GEB a (MeV)

b= GEB b (MeV^{1/2})

E= peak energy (MeV)

The solutions ‘a’ and ‘b’ were applied to the GEB function in the MCNPX simulation. Because the several simulations about each detector were required to analyze the peaks, the efficient distribution of simulation time was needed. For this reason, the unit of minimum fraction was set as the 10 keV energy bin for the spectrum results by the simulation. The Table 1 shows two GEB values of each detector material, as well as the list of detectors including the density and the average energy resolution values (511 keV and 662 keV) for the simulations. The average energy resolution was acquired by the average calculation using the extracted energy resolution from other research [10-26]. Thus, the energy resolution values in the Table 1 could not be absolute representative values because of the influence by many factors. After the setting of the GEB values, the prompt gamma ray energy spectra were acquired using the F8 tally. To obtain a more correct energy spectra from the simulations, an artificial virtual

target (components: carbon (12C): nitrogen (14N): oxygen (16O) = 1:1:1, density = 3.0 g/cm³, size = 5 cm × 5 cm × 5 cm) was used. In order to induce the active reaction with the target, a 14.1 MeV neutron flux was directed toward the target, and the detectors surrounded the target. The setting of neutron flux (2×10^{10} n/sec) for the MCNPX simulation was referred from the reference research [4].

The prompt gamma ray energy spectra induced by the 14.1 MeV neutrons are shown in Figs. 2(a)-(f). The spectra showed characteristic prompt gamma ray energy peaks regarding the intrinsic atoms of the target material. Each peak corresponds to a specific prompt gamma ray energy values (12C: 4.43 MeV, 14N: 1.64, 2.31, and 5.11 MeV, 16O: 2.73, 3.69, 5.11 (double escape peak from 6.13 MeV (16O)), 6.13, 6.92, and 7.12 MeV). The energy resolutions at these nine peaks were calculated for the eighteen different detectors.

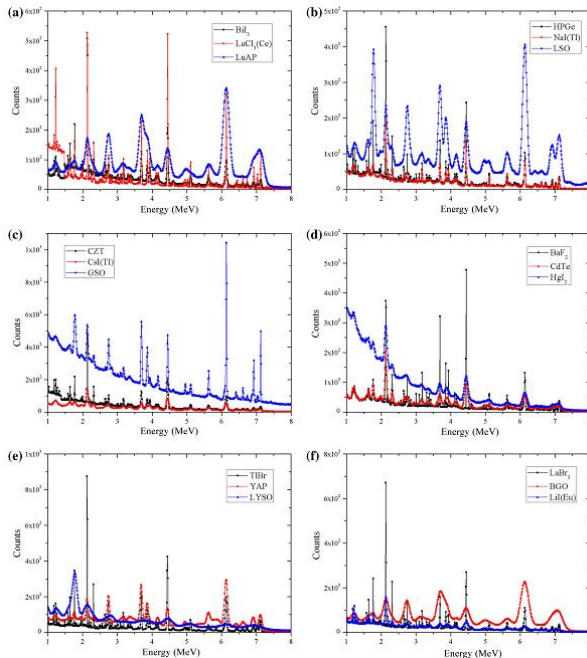


Fig. 2. The Monte Carlo n-particle extended (MCNPX) simulations of the eighteen different prompt gamma ray energy spectra. Line colors depending on energy resolution level were assigned to energy spectrum of each detector in the group. The group of good resolution was demonstrated as the black line (top of legend), the red line (middle of legend) shows mid-level resolution group and the blue line (bottom of legend) shows poor level resolution group. (a) BiI₃, LaCl₃(Ce) and LuAP, (b) HPGe, NaI(Tl) and LSO, (c) CZT, CsI(Tl) and GSO, (d) BaF₂, CdTe and HgI₂, (e) TlBr, YAP(Ce) and LYSO, (f) LaBr₃(Ce), BGO and LiI(Eu) detector materials [5].

In order to discriminate the peak from the spectrum, the calculation of the FWHM (energy resolution) regarding each peak was performed many times. In this study, the ten iterative calculations per one peak were

conducted to conclude the energy resolution. The representative value of energy resolution was set using the average value of these ten calculated values.

The result of the number of discriminated peak depending on the detector material is shown in Fig. 3(a). The CZT, HPGe, BaF₂, TlBr, BiI₃ and LaBr₃(Ce) distinguished all nine peaks with good energy resolution values (energy resolution < 1.5%) through the ten iterative calculations. The fluctuation of the number by the ten iterative calculations was observed as the maximum six counts. The method of grouping for the graphs (Figs. 2(a)-(f)) were based on the number of discriminated peak from the Fig. 3(a). The six detectors which discriminated all nine peaks were assigned as 'good resolution' line to each group. And the six detectors which were reported as low count number (< 4) were assigned as 'poor level resolution' line to each group. Because only energy resolution was considered to classification of detectors according to their performances, an absolute data of a detector's comprehensive performance cannot be given. The significances of the relationships between the reaction cross-sections of each atom reacting with the neutron and the ratio of discriminated peak from all the detectors are shown in Fig. 3(b). The black line means the level of the reaction cross-section (%) depending on the atom. The reaction cross-section values of the oxygen, the carbon, and the nitrogen were 100%, 95%, and 85%, respectively (source from NIST). The discrimination probability of the peak from 18 detectors at the nine peak points was defined using the number of the discriminated peak (the red line). In case of the red line, the maximum fluctuation of values was 55% at the 5.11 MeV energy peak during the ten iterative calculations. If the two peaks which are induced by the different source were overlapped at the same energy level in the spectrum, there were many changes of the number of 'None' case. The 6.13 MeV peak from the oxygen and the 4.43 MeV peak from the carbon were perfectly discriminated from all the detectors. However, the 5.11, 6.92, and 7.12 MeV peaks were discriminated as the lowest level. Because the difference between the 6.92 MeV and the 7.12 MeV is only 0.2 MeV, if the detector has the enough capacity of the discrimination, the two peaks can be discriminated easily. Averagely, when the energy resolution of the detector is below 2.8% at the 7 MeV, the occurrence of 'None' case is easy.

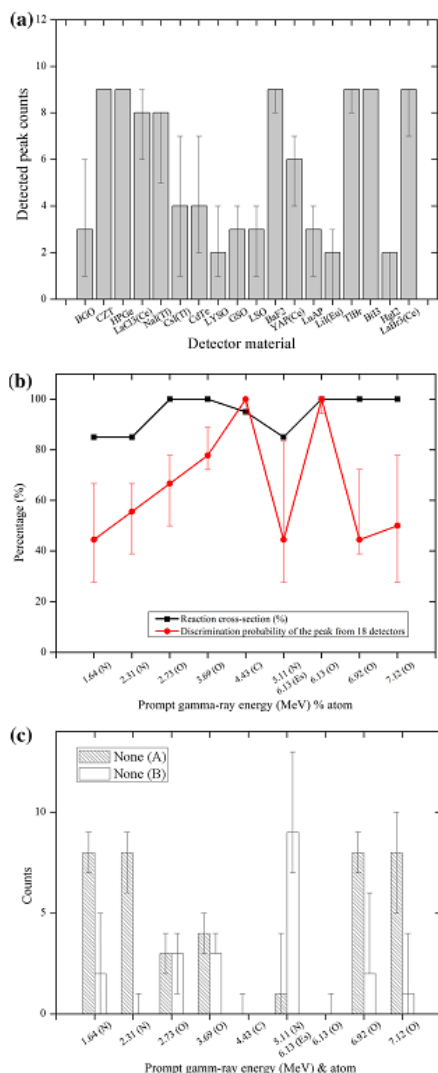


Fig. 3. Analysis of the peak discrimination and trend from the energy resolution results [6]. (a) Detected peak counts number according to the detector material (average counts by the ten iterative calculations, uncertainty: maximum 6 counts), (b) The comparison of reaction cross-section with discrimination probability of the peak (average values by ten iterative calculations, maximum fluctuation rate: 55%), (c) Counting of 'None (A)' and 'None (B)' at the nine peak points (average values by ten iterative calculations, uncertainty: maximum 6 counts).

3. Conclusions

To the best of our knowledge, the results in this study are the first reported data regarding the peak discrimination of high energy prompt gamma ray using the many cases (the eighteen detector materials and the nine prompt gamma ray peaks). The reliable data based on the Monte Carlo method and statistical method with the identical conditions was deducted. Our results are important data in the PGAA study for the peak detection within actual experiments.

REFERENCES

[1] I. Jun , W. Kim, M. Smith, I. Mitrofanov, M. Litvak, A study of Venus surface elemental composition from 14 MeV neutron induced gamma ray spectroscopy: activation analysis, Nucl Instrum Method Phys Res A, Vol. 629, pp. 140–144, 2011.
 [2] C. Eleon, B. Perot, C. Carasco, Preliminary Monte Carlo calculations for the UNCOSS neutron-based explosive detector. Nucl Instrum Method Phys Res A, Vol. 619, pp. 234–239 2010.
 [3] S. Jakhar, C. Rao, A. Shyam, B. Das, Measurement of 14 MeV neutron flux from DT neutron generator using activation analysis, IEEE Nucl Sci Symp Conf Rec, pp. 2335–2338, 2008.
 [4] M. McClish, P. Dokhale, J. Christian, C. Stapels, E. Johnson, F. Augustine, K.S. Shah, Performance measurements from LYSO scintillators coupled to a CMOS position sensitive SSPM detector, Nucl Instrum Method Phys Res A, Vol. 652, pp. 264–267 18, 2011.
 [5] J. Trummer, E. Auffray, P. Lecoq, A. Petrosyan, P. Sempere-Roldan, Comparison of LuAP and LuYAP crystal properties from statistically significant batches produced with two different growth methods, Nucl Instrum Methods Phys Res A, Vol. 551, pp. 339–351, 2005.
 [6] A. Owens, A. Peacock, Compound semiconductor radiation detectors, Nucl Instrum Method Phys Res A, Vol. 531, pp. 18–37, 2004.